**ATS/Note/2011/075 (TECH)**

2011-09-09

Fritz.Caspers@cern.ch

# A novel type of forward coupler slotted strip-line pickup electrode for non-relativistic particle beams

F. Caspers/ BE-RF-BR

Stochastic cooling, Schottky signals, pick-up, kicker, low beta beam

**Summary**

A novel type of slotted or perforated strip-line pick-up or kicker electrode structure for non-relativistic particle beams with $\beta=v/c$ values around 0.7 is presented. This slotted structure is to be used as a forward coupler with the output signal taken from the downstream end and has a rather large relative bandwidth of several octaves. Possible applications are stochastic cooling systems e.g. for ions beams in the momentum range mentioned above. This electrode may also be used for Schottky diagnostics.

## 1. The conceptual model of a multi-slot strip-line electrode

A photo and a schematic drawing of the slotted electrode is shown in Fig.1. The unit cell length (b) is 12 mm and the thickness (t) of the electrode metal foil amounts to 0.15 mm. A large number of small slots in this electrode (total width = $a$, total length = $L$) provide distributed inductive loading, slowing down the phase velocity of the travelling wave structure. This very first model shown in Fig. 1 had already been designed and produced at CERN in 1998 for tests of the concept but was left dormant for about a decade until interest from IMP CSR (Lanzhou) showed up recently. The reduction in phase velocity is a function of slot length ($c$), slot width ($d$), electrode thickness, and the spacing between electrode and ground. From the measurement and simulation results it is evident that up to 1.5 GHz this structure has very low phase dispersion. In contrast to other similar looking electrodes (Faltin type pick-up [1], McGinnis type slotted waveguide structure [2] for $\beta$=1) this device is very broadband, operating from low frequencies upwards as a forward coupler. Reduction of phase velocity for strip-line type electrodes can also be achieved by dielectric loading, but there is a penalty in terms of sensitivity. Examples of low-$\beta$ structures with dielectric loading are printed meander lines on a dielectric substrate [3]. Obviously in addition to the downstream signal which augments proportionally with the square of the electrode length, the signal available at the upstream end may be used for additional diagnostic purposes. Advantages of the proposed structure are the simple and cheap construction as well as low mechanical height. This low height permits installation where vertical aperture is an issue, e.g. in a bending magnet. This kind of inductive loading, using a large number of rather small slots is applicable for a $\beta$-range from about 0.5 to 0.95. Due to the small size of the slots the frequency dependence of the inductance of these slots is very low, thus leading to a small dispersion over a large frequency range

Electrode thickness: 0.15 mm, gap between electrode and ground: 1.5 mm

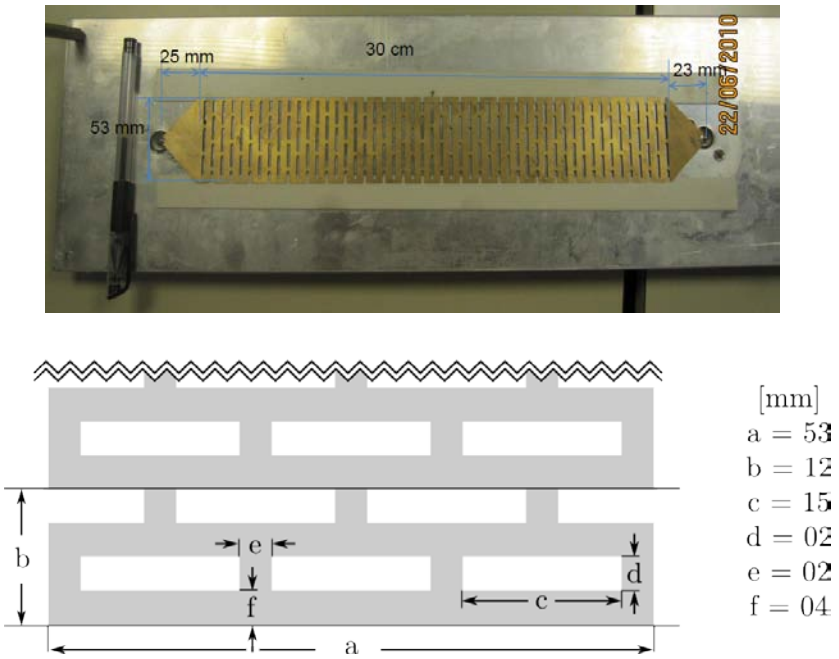


**Figure 1:** The multi-slot strip-line electrode. The total number of cells in this example is 25.

## 2. Simulation and measurement results

### 2.1 Phase dispersion and phase velocity data

A comparison of measurement and simulation results is shown in Fig. 2. We notice that the phase dispersion is rather small and the deviation from linear phase (displayed in Fig. 2) amounts only 11 degrees at a frequency of 1.5 GHz for a 30 cm long structure (length of the elementary cell $b$=12 mm). Fig. 3 shows the simulated results for the phase dispersion when the electrode has 40 cells ($L$=0.48 m long electrode) or 80 cells ($L$=0.96 m long electrode). The phase deviation is 24 degrees at 1.5 GHz for 80 cells and thus is still not very large. Thus in a frequency range from a few MHz to 1.5 GHz this structure has a phase dispersion acceptable for many applications.

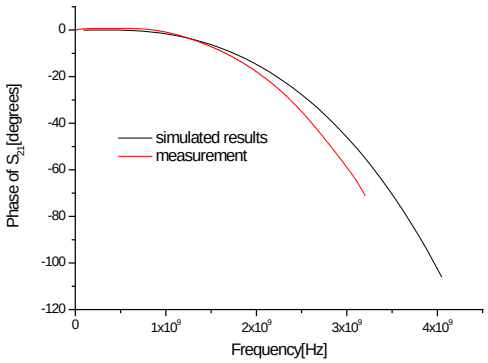


**Figure 2:** Phase of $S_{21}$ for 25 cells. The black line shows the simulated and the red line the measured results.

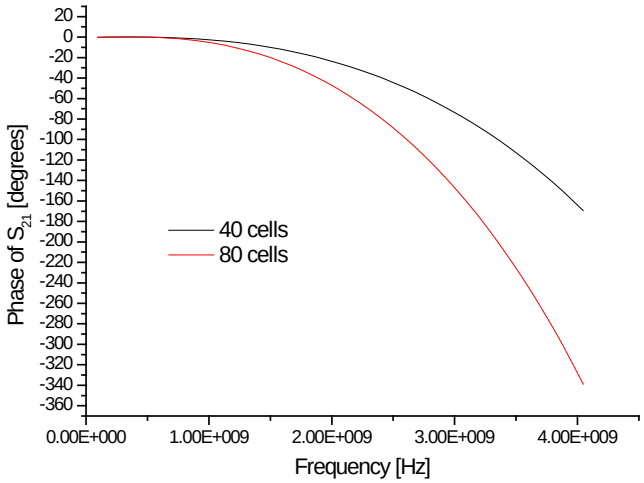


**Figure 3:** Phase dispersion for 40 cells (black line) and 80 cells (red line).

For this type of electrode, the phase velocity is determined by the slot size, thickness of the electrode and the distance from the electrode to ground. When increasing the thickness of the metal strip and its distance to the ground plane the phase velocity rises as well. In the measurement the phase velocity can be deduced from the phase $\Phi$ of the complex transmission coefficient $S_{21}$ or alternatively in the time domain from the travel time $\tau$ (Fig. 4) by the relation given in Eqn. 1.

$$\beta = \frac{2\,L}{c\,\tau} \qquad \tau = \text{round-trip travel time} \tag{1}$$

$L$ stands for the electrode length. The agreement between both results is good. Minor deviations are partly related to the interpretation of measurement data, both in the time and frequency domain.

## 2.2 Characteristic impedance and electrical length from time domain measurements

Fig. 4 shows the step response in real time obtained with a Lecroy sampling scope where the characteristic impedance returns as about 17 Ohm, which is nearly equal to the simulated result obtained from CST MWS (Figure 5). The variation of the characteristic impedance versus spacing *s* between electrode and ground is also depicted in Fig. 5.

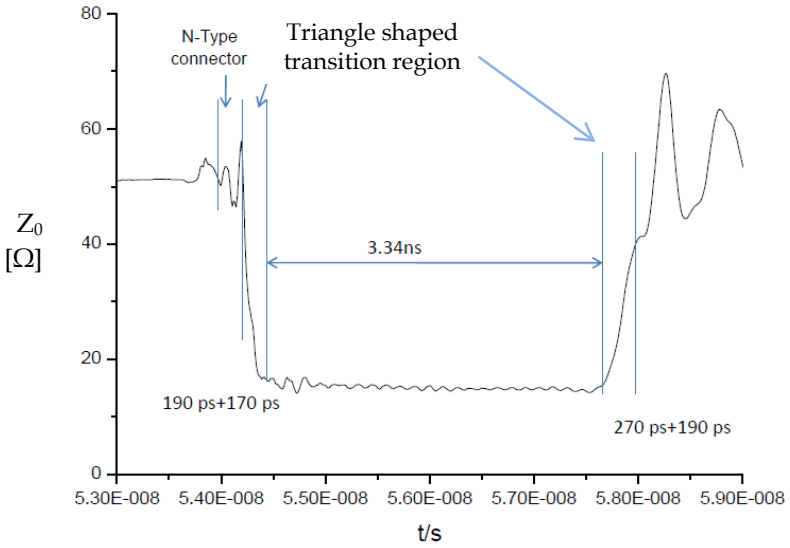


**Figure 4:** Impedance measurement results using the TDR (Time Domain Reflection) method on a 30 cm long model

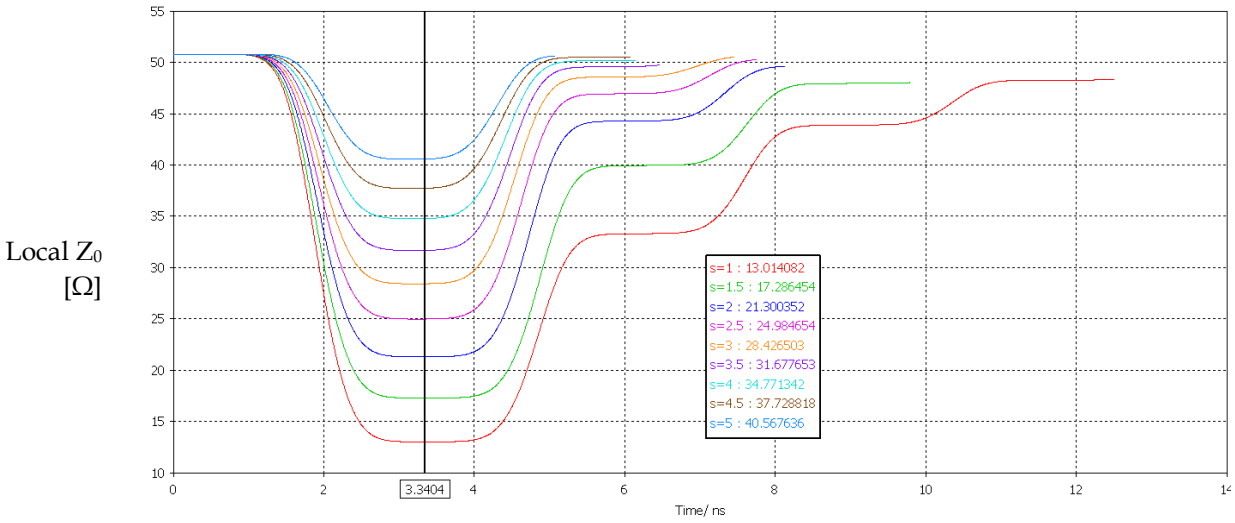


**Figure 5:** Simulated results of characteristic impedance for different *s*= distance electrode to the wall

A precise determination of the phase velocity for this 30 cm long model from TDR data is not really possible in a straightforward manner with this method due to the impact of transition sections and connectors. Using Eqn. (1) we would obtain a $\beta$-value very close to 0.6. But one has to keep in mind that for this 300 mm long model with transition tapers of 25 mm length *and* coaxial feed-throughs on either side the rising slope of the step-function (Fig. 4) is likely to be shifted by about 5…10% with respect to the true electrical length of the slotted region. Resonator type measurements (with corrections for the taper) indicate $\beta$-values around 0.65 for this 53 mm wide structure (first measured $\lambda/2$ resonance at ≈ 300 MHz).

# 3. Example of a prototype pickup electrode in the vacuum chamber of a bending magnet

## 3.1 Electrode structure

A photograph and a technical drawing of the perforated electrode are shown in Fig. 6. Five slots ($c$=15mm by $d$=2 mm) are positioned across the width of the pick-up/kicker metal strip. The unit cell length amounts to $b$=12 mm and the thickness of the electrode is 0.4 mm. The electrode which follows the bending of the vacuum chamber inside the bending magnet is $a$=87 mm wide and about $L$=1 m long.

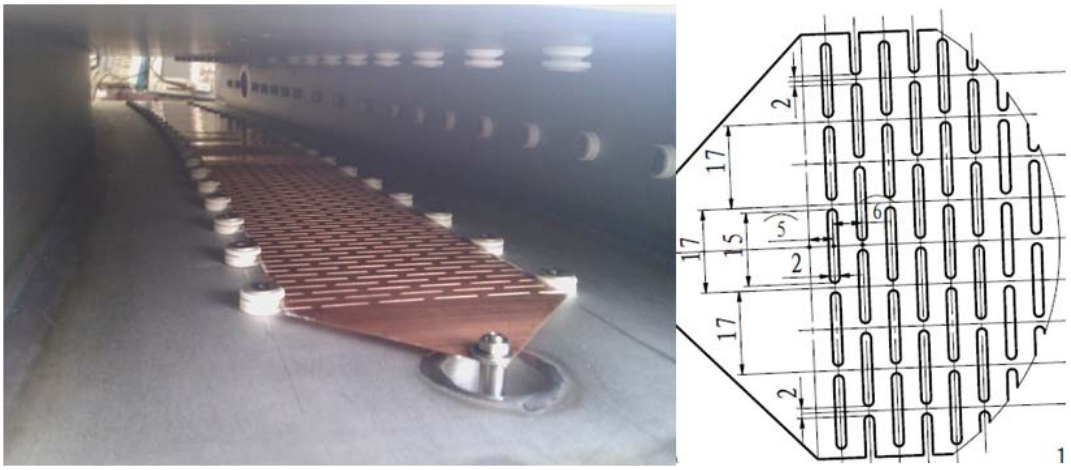


**Figure 6:** The slotted structure of travelling wave mode with number of cells = 80 and the length L ≈ 1 meter

## 3.2 Simulation and measurement results in the frequency domain

The phase response of the measurement is shown in Fig. 7. The phase difference from the linear phase (with subtracted delay term) is not more than 45 degrees at 1.5 GHz for the nearly 1 m long electrode. The measured (network analyzer) and simulated results (CST MWS) are compared as well, as shown in Fig. 8. For frequencies below 1.5 GHz the agreement is reasonable.

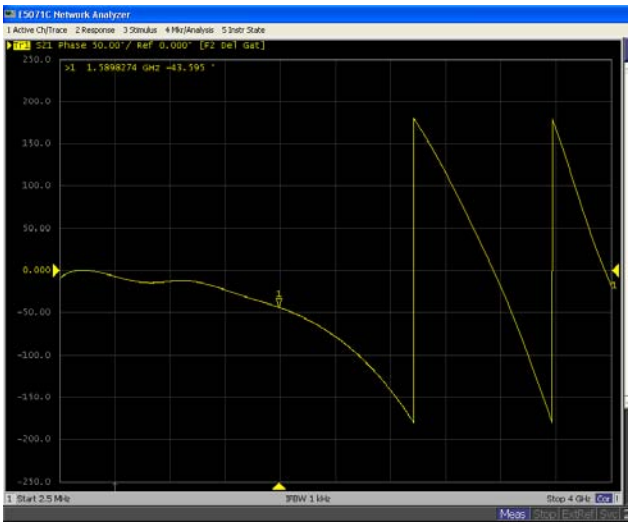

**Figure 7:** Phase of $S_{21}$ for 80 cells

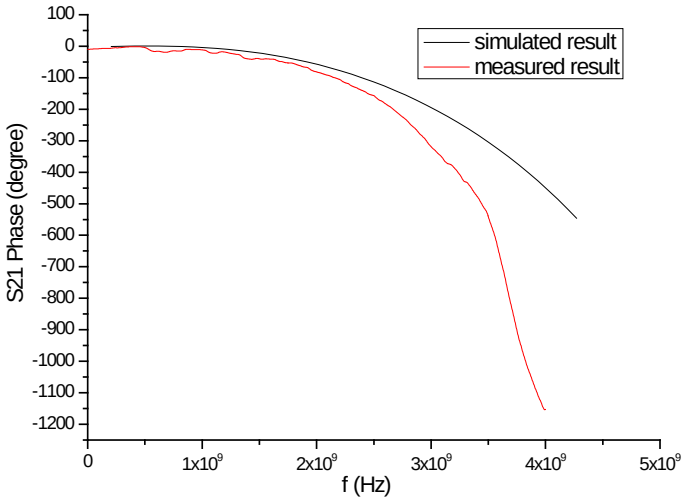


**Figure 8:** Comparison of $S_{21}$ between measured and simulated result

The phase velocity is measured using the resonant method by replacing the connection of the electrode on both ends to the inner conductor of the measurement lines by (weak) capacitive coupling [4], i.e. positioning the pin of the feed-through very close to the electrode but leaving it unconnected. The measured results (S-parameter data) are depicted in Fig. 9.

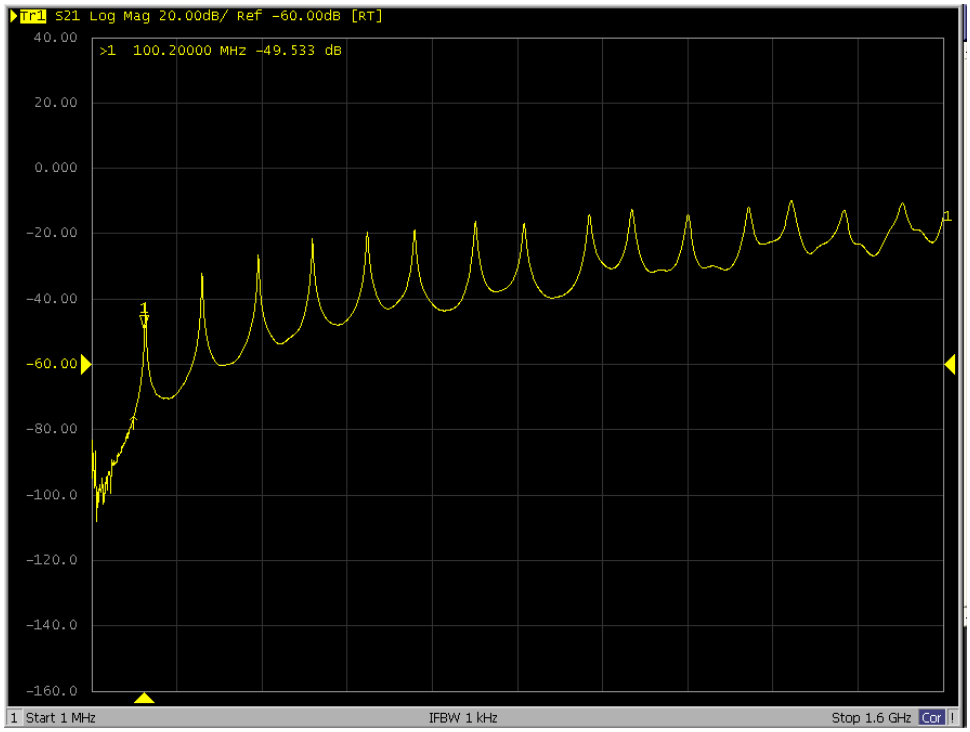


**Figure 9:** Resonant measurement result of the electrode

From the resonant frequency and $Q$ value, the phase velocity and the attenuation of the electrode can be calculated using Eqn. (2) and Eqn. (3),

$$\beta = \lambda \frac{f}{c} = \frac{2L}{n} \frac{f}{c} \tag{2}$$

$$\alpha = \frac{n}{2L} \frac{\pi}{Q} \left[\frac{Np}{m}\right] = \frac{n}{2L} \frac{\pi}{Q} 8.686 \left[\frac{dB}{m}\right] \tag{3}$$

Where $n$ is the resonant harmonic and $L$ is the electrode length, which is 1.03 m. The results for the phase velocity and attenuation are shown in Table 1. The phase velocity is roughly about 0.7, which is not too far away from the simulated result obtained with CST MWS, as shown in Fig. 10.

**Table 1:** Beta and attenuation result

| $n$ | $f$ (MHz) | $Q$ | $\beta$ | Attenuation (dB/m) |
|---|---|---|---|---|
| 1 | 101.66 | 110 | 0.69806 | 0.12036 |
| 2 | 208.36 | 138 | 0.71537 | 0.19188 |
| 3 | 314.20 | 157 | 0.71917 | 0.25299 |
| 4 | 415.80 | 163 | 0.71379 | 0.32490 |
| 5 | 518.48 | 163 | 0.71205 | 0.40613 |
| 6 | 607.66 | 171 | 0.69543 | 0.46455 |
| 7 | 722.04 | 172 | 0.70829 | 0.53883 |
| 8 | 812.94 | 167 | 0.69777 | 0.63424 |
| 9 | 935.06 | 164 | 0.71342 | 0.72657 |
| 10 | 1016.00 | 145 | 0.69765 | 0.91309 |
| 11 | 1120.70 | 144 | 0.69959 | 1.01137 |
| 12 | 1234.00 | 140 | 0.70612 | 1.13484 |
| 13 | 1315.00 | 113 | 0.69459 | 1.52316 |

The interpretation of these measured results requires a certain amount of caution. Of course the resonance frequencies are very well defined but defining the correct effective length of the electrode is not straightforward. The geometrical length between the ends amounts to 106 cm, including triangular transition sections. Distributing the capacitance of these transition regions from a triangle to a strip with the full with of the electrode returns an effective length of 103 cm.

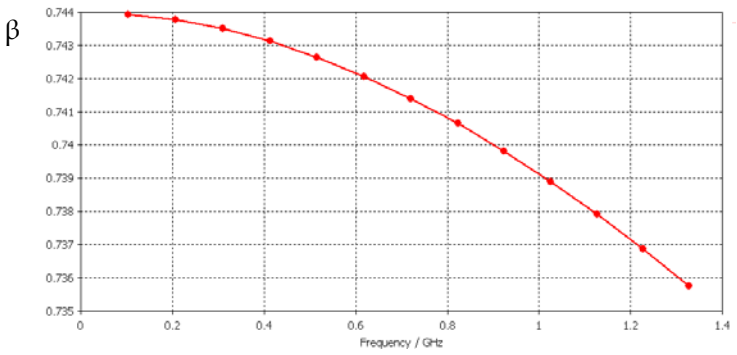


**Figure 10:** Simulated result for the phase velocity

## Acknowledgements

The author would like to thank Junxia Wu and Y. Zhang from Lanzhou IMP (CSR) for having provided the numerical results and measurement plots, produced in close collaboration during a visit to Lanzhou in summer 2011. Many thanks belong to IMP Lanzhou for the warm reception and generous hospitality during a working week in summer 2011. The support by the CERN-BE management for this collaboration is highly appreciated and thanks to D. Möhl and E. Ciapala for heaving read and corrected the manuscript. A more detailed description of the methods and results obtained will be given in forthcoming papers.

## References

[1] L. Faltin, Slot-type pick-up and kicker for stochastic beam cooling; NIM 148, p. 449-455, 1987

[2] D. McGinnis, Slotted waveguide slow-wave stochastic cooling arrays; proc. PAC99

[3] N. Tokuda, Travelling wave pickups and kickers for stochastic cooling at low beam velocity; 4th LEAR Workshop, Villars-sur-Ollon, Switzerland, 6 - 13 Sep 1987, pp.135-138

[4] T. Kroyer, F. Caspers, E. Gaxiola, Longitudinal and transverse wire measurement for the evaluation of impedance reduction measures on the MKE extraction kickers, AB-Note-2007-028